PHOTOCHEMICAL BEHAVIOR OF NITROPHENOLS AT AEROSOL INTERFACES

W. Churchill Wilkinson, B.S. in Chemistry with Honors, William & Mary
Advised by Dr. Nathanael Kidwell, William & Mary Department of Chemistry

Abstract

The solar absorption outcomes of brown carbon (BrC) aerosols are a primary subject of investigation in atmospheric chemistry due to their impact on climate, atmospheric composition, and human health. BrC efficiently absorbs ultraviolet and visible wavelengths, opening a complex set of photochemical pathways. Many of these photochemical processes occur at the air/aerosol interface, where partial solvation geometries facilitate unique, often accelerated chemistry. Nitroaromatic compounds have been identified as important chromophores in BrC aerosols. This study investigates the fundamental geometry and molecular motion of *ortho*-nitrophenol, a prototypical BrC nitroaromatic compound, at aerosol interfaces using the powerful surface-selective spectroscopic technique vibration sum-frequency generation (VSFG) spectroscopy. Experimental data is complemented with high-level density functional theory calculations used to obtain the spatial geometries and hydrogen bonding networks of *ortho*-nitrophenol at an interfacial solvation environment. Overall, results provide insights into likely conformational and spectroscopic properties of *ortho*-nitrophenol at the air/aerosol interface.

Introduction

Aerosol, also known as particulate matter (PM), is a fine suspension of liquid or solid matter in the atmosphere and is of interest in environmental science due to its myriad environmental effects. There are numerous types of aerosols, from salty sea spray aerosol to particulate matter produced from volcanic eruptions. A large fraction of aerosol is made up of organic molecules and is classified as organic aerosol (OA).[1] OA exerts significant impact on climate, atmospheric composition, and human health, making it a major subject of investigation in atmospheric chemistry. An area that still requires much research is the role of OA in radiative forcing. OA can either absorb solar radiation and impose a warming effect (positive forcing) or scatter light and have a net cooling effect (negative forcing).[1] White carbon aerosols are particulates that predominantly scatter light, whereas black carbon aerosols absorb solar radiation over a large spectral range from ultraviolet to infrared wavelengths. Relatively recently, a type of organic aerosol dubbed brown carbon (BrC) has been identified. This type of OA contains chromophores that absorb near-UV (300-400nm) and visible wavelengths particularly well and is thus of interest due to the unique photochemical properties afforded by this absorption profile.[1] However, further investigation is needed to fully understand the solar absorption outcomes and thus the environmental impacts of BrC aerosol.

This study seeks to understand the behavior of this molecule at the surface of aerosol particles. The air/aerosol interface is the locus of many chemical processes important to atmospheric chemistry. OA particles often contain aqueous environments, so organic chromophores at their surfaces experience unique solvation geometries that have been shown to fundamentally change photochemical outcomes. In fact, there is evidence demonstrating that certain photochemical processes, such as the photodissociation of phenol to produce a hydrogen atom, electron, and phenoxy radical become greatly accelerated at the

air/aerosol interface.[2] Thus, the interfacial behavior of important organic chromophores such as *ortho*-nitrophenol (oNP) is essential for gaining a molecular understanding of how BrC aerosol interacts with solar radiation and how these interactions might drive atmospheric composition and climate. In particular, the aim of this study is to elucidate the interfacial photochemical behavior of oNP, a nitroaromatic molecule that has been identified as an important constituent of BrC aerosol, in aqueous aerosol particles.[1] This will be accomplished through the synergy between high level theoretical calculations and detailed, interface-specific spectroscopic information.

Methods

Vibrational sum frequency generation (VSFG) spectroscopy was used in the study of the interfacial behavior of nitrophenols. This nonlinear spectroscopy technique involves focusing two high intensity lasers onto the interface between two media and detecting a third photon, called the sum-frequency generated (SFG) photon because its frequency is the sum of the frequencies of the first two photons, which is created from the first two lasers interacting with the molecules at that interface. As shown in Figure 1, the IR photon vibrationally excites the molecule and the visible photon further excites the molecule to a short-lived virtual state. The relaxation of the molecule results in the emission of an SFG photon.[3] Before discussing the experimental methods involving VSFG that were used in this study, it is instructive to discuss the theory behind the technique.

VSFG spectroscopy is useful to those interested in interfacial chemistry because the physical process it detects can only occur at an asymmetric environment like the interface between two media. Like all spectroscopic techniques, including the ones previously

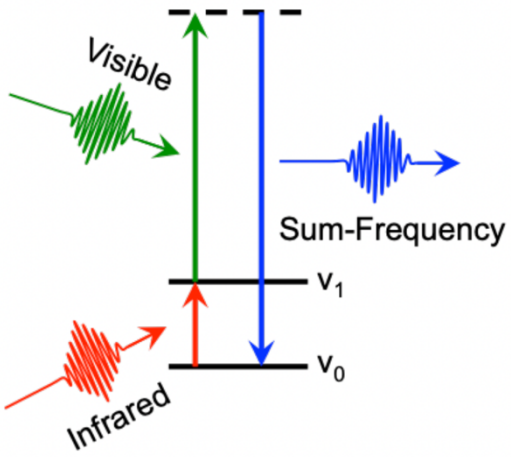

***Figure 1**: Energy level schematic of VSFG Spectroscopy showing the IR and visible photons exciting the molecule and the resulting sum-frequency generated photon.*

mentioned here, VSFG involves a particular type of light-matter interaction. When a medium is exposed to light, the light's electric field propagates through the material and induces a dipole. For low-intensity, incoherent light, this light-induced dipole increases linearly with the magnitude of the light's electric field. When these individual induced dipoles are summed, one can obtain the bulk polarization ($\vec{P}$) of a material, or the polarization per unit volume. When high-intensity, coherent light is incident on a material, such as when a material is struck with laser radiation, the response of the material to the light can no longer be described linearly and now includes higher-order terms. VSFG involves irradiating a medium with two lasers at once, so the response of the material based on two propagating electric fields is of interest. The bulk polarization of a material under two incident light sources, or the second-order bulk polarization, is defined by the equation

$$\vec{P}^{(2)} = \varepsilon_0 \chi^{(2)} \vec{E}_1 \vec{E}_2$$

where ε_0 is the vacuum permittivity of free space, $\chi^{(2)}$ is the second-order susceptibility of

medium, and $\vec{E}_1$ and $\vec{E}_2$ are the electric fields of the two light sources. The electric field induced in the material will oscillate at a frequency that is the sum of the frequencies of the two original electric fields; in VSFG spectroscopy, the energy of the output photon will be the sum of the energies of the two input photons.[3] VSFG spectroscopy is interface specific because $\chi^{(2)}$ is only nonzero within media that do not have inversion symmetry. In the bulk of a material, the positions of the molecules are random and average to form an isotropic, centrosymmetric environment that possesses inversion symmetry. On the other hand, molecules at the surface of a material have anisotropic orientations, so there is no inversion symmetry at the interface, allowing sum frequency generation to occur.[3]

Illustrated in Figure 2, VSFG spectroscopy was used in this study to probe the interfacial vibrational modes of nitrophenols sitting at the oil/H_2O and oil/D_2O interfaces, proxies for the aerosol interface. The oil used in the experiment was carbon tetrachloride (CCl_4). In the experiment, an IR laser and a visible light laser (532 nm) are overlapped both spatially and temporally on the interface between the oil and the H_2O (or D_2O) where interfacial nitrophenol molecules are present. 2-Nitrophenol and 4-nitrophenol were interrogated in individual experiments and were added at 1mM and 10mM concentrations, respectively. Both laser light sources were generated using a harmonics unit along with an OPO/OPA/Difference frequency generation system pumped by a picosecond Nd:YAG laser.

The two lasers interact at the interface and produce a sum-frequency generated photon which exits the sample container and enters a monochromator paired with a photomultiplier tube (PMT) for detection. The IR laser is scanned across a spectral region and the visible laser is fixed so that it will not electronically excite the molecule of interest. When the IR laser is resonant on a vibrational transition within the molecule, there is an enhancement of the sum frequency generated light at the interface which is detected by the PMT.

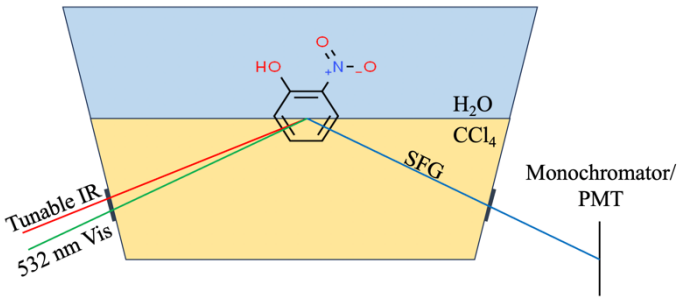

***Figure 2**: Illustration of the sample holder and the process by which the IR and visible beams excite the target molecule at the oil-water interface to form an SFG photon.*

The resulting VSFG spectrum corresponds to the wavelengths of IR light that induce this enhancement of SFG and represents the *interfacial* vibrational spectrum of the molecule of interest. In this study, the IR laser was scanned from 2500-3700cm^{-1} to capture C—H, O—H, and O—D vibrational modes within the nitrophenols and interfacial solvent molecules. Importantly, a vibrational mode must be both infrared and Raman active to be VSFG-active. Additionally, the polarization of the laser beams can be altered to probe different orientations of molecules at the interface.

Computational Methods

Since the nitrophenol study regards the behavior of nitrophenols at interfaces between water and some other medium, the aim of the computational portion of the study was to determine how nitrophenols behave when partially solvated with a finite amount of water molecules (n = 1-5). This involved two steps: (i) an ABCluster conformational search and (ii) optimized geometry and vibrational frequency calculations using Gaussian 16. ABCluster, which utilizes the Artificial Bee Colony algorithm, was used to sample the conformational space of 2-nitrophenol and 4-nitrophenol clustered with 1-5 water molecules to generate a list of 200 candidate isomers.[5] Since ABCluster operates using molecular

force fields, a relatively weak type of theoretical simulation, each candidate structure was then subjected to a density functional theory geometry optimization and vibrational frequency calculation at the ωB97XD/6-311++G(d,p) level of theory using Gaussian 16 to further optimize the candidate isomers.[4] This produced a final list of 200 optimized molecular clusters with vibrational modes computed. The directory for each cluster (2 and 4-nitrophenol with 1-5 H_2O molecules) was then sorted by their total zero-point-corrected electronic energies to determine the lowest energy conformations and their corresponding vibrational modes. Structures and vibrational modes were visualized using the GaussView 6 software. All theoretical calculations were carried out on the William & Mary High Performance Computing SciClone Cluster.

Results and Discussion

Optimized oNP:nH_2O Geometries

To analyze the interfacial behavior of nitrophenols, having approximations of their geometries when solvated with a finite number of water molecules is paramount. To this end, ABCluster and Gaussian calculations were performed. Figure 3 shows the lowest energy geometry for each oNP:nH_2O (n=1-5) cluster yielded from the computational process. Additionally, a theoretical vibrational spectrum was produced for each cluster, which will be discussed below. Due to their role in controlling the chemical behavior of the system, there are two central geometrical features of these structures that are of interest: the hydrogen bonding network and the out-of-plane rotations of the nitro (NO_2) and hydroxyl (OH) functional groups. Recall that the lowest energy conformational isomer of oNP is entirely planar, making the quantification of the geometrical perturbation very simple. The functional group rotations will be quantified using dihedral angles.

It is well-characterized that water can act as a hydrogen bond donor and acceptor, allowing it to form large networks containing strong noncovalent interactions. Examining the presence of hydrogen bonding networks for partially solvated nitrophenols provides a wealth of information regarding how nitrophenols interact with their solvation environment at the surface of aerosol particles. Furthermore, the out-of-plane rotation of functional groups on the nitrophenol caused by the presence of water molecules in these clusters can inform the impact of the interfacial solvation environment on certain

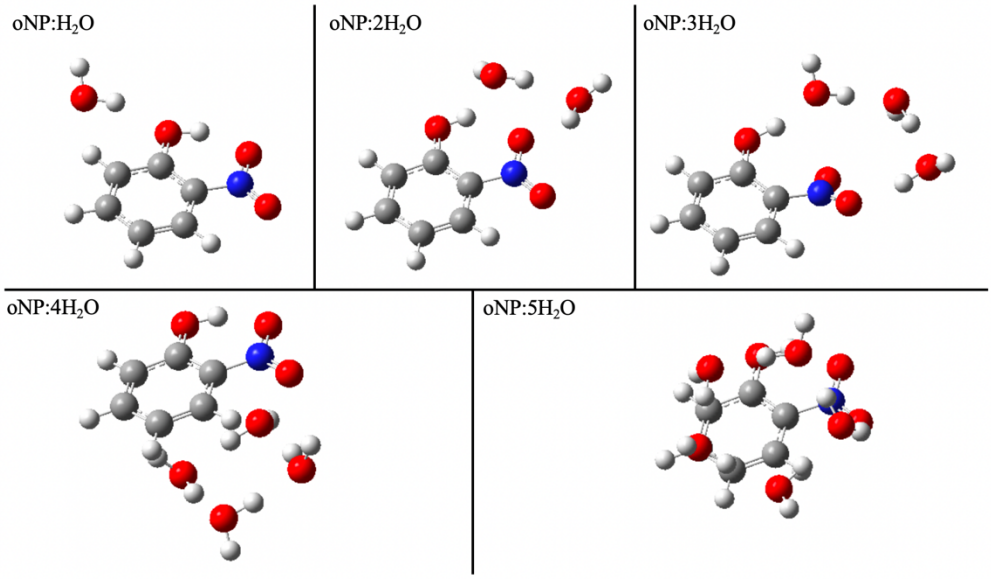

***Figure 3**: Structures for oNP:nH_2O (n=1-5) yielded from the two-step computational process.*

photochemical processes that nitrophenols can undergo.[6]

In the oNP:H_2O complex, the optimal position for the one water molecule is adjacent to the hydroxyl group of the nitrophenol acting as a hydrogen bond donor. This implies that this is the strongest hydrogen bond that a single water molecule could form with the chromophore. Additionally, the oNP functional groups are minimally rotated out of the plane of the aromatic ring. In oNP:$2H_2O$, the two water molecules hydrogen bond with each other, with one acting as a hydrogen bond acceptor with the H-atom in the oNP –OH group and the other water molecule acting as a donor to the O-atom in the $–NO_2$ group. With two water molecules present, the formation of a hydrogen bonding network is already observed. The two functional groups are more rotated in oNP:$2H_2O$ than in oNP:H_2O, but only minimally so.

oNP:$3H_2O$ possesses the most unique geometry of the optimized clusters. The hydrogen bonding network is very similar to that of oNP:$2H_2O$, but the additional water molecule has been placed between the two water molecules interacting with the nitrophenol, expanding the network of intermolecular interactions. What is notable about this cluster compared to the others is the strong perturbation to the oNP geometry caused by the three-water hydrogen bonding network. The ON-CC dihedral angle, which corresponds to the rotation of the $–NO_2$ group, is -28.208° and the HO-CC dihedral angle, which corresponds to the rotation of the –OH group, is -21.774°, indicating that the two functional groups are rotated out of the plane of the aromatic ring an order of magnitude more than in any of the other clusters, showing that the intermolecular interactions involved in the hydrogen bonding networks lead to strong geometrical perturbations in oNP.

oNP:$4H_2O$ and oNP:$5H_2O$, which will be referred to as the "higher order" clusters, exhibit similar behavior and will thus be considered simultaneously. The structure of oNP in these clusters is far less perturbed than in oNP:$3H_2O$ since the waters congregate into a cyclical hydrogen bonding network that sits roughly in plane with the aromatic chromophore. In the $4H_2O$ cluster, the waters form a square network, and the $5H_2O$ cluster possesses a pentagonal network. This behavior demonstrates that, at least under the level of theory used, when four and five water molecules are present, the cyclical hydrogen bonding network formed between the water molecules is more stable than a network that directly involves the chromophore.

NCIPlot Results

Further analysis of the theoretical oNP:nH_2O geometries was conducted using NCIPlot, a software capable of creating visualizations characterizing the spatial characteristics and strength of the noncovalent interactions within a system.[7] When functional groups engage in inter or intramolecular noncovalent interactions, their electron clouds experience a perturbation. These perturbations create a region of small electron density between the moieties participating in the interaction. NCIPlot detects these regions and computes various quantities pertaining to the spatial topology and magnitude of electron density to characterize noncovalent interactions as either strong stabilizing interactions (e.g., hydrogen bonding), strong repulsive interactions (e.g., steric crowding), or weak stabilizing interactions (e.g., Van der Waals forces). The program then generates plots containing surfaces that represent these interactions. Strong stabilizing surfaces are blue and spatially compact whereas weak stabilizing surfaces are green and spatially diffuse. Strong repulsive surfaces are represented as red, and while they provide important information about chemical systems, they are of slightly less interest in this study.[7]

NCIPlot renders were created to visualize the noncovalent interactions in each of the optimized oNP:1-$5H_2O$ clusters. More

specifically, the renders provide further insight into the nature of the hydrogen bonding networks present in the complexes. Shown in Figure 4 are the NCIPlot renders for oNP:1-5H_2O clusters, but the plots for oNP:3H_2O and oNP:4H_2O are generally representative of those found in the lower and higher-order clusters respectively, except for the intramolecular hydrogen bond between the hydroxyl and nitro groups of oNP, which is present in all but 3H_2O where the geometry does not allow for this interaction. In fact, the

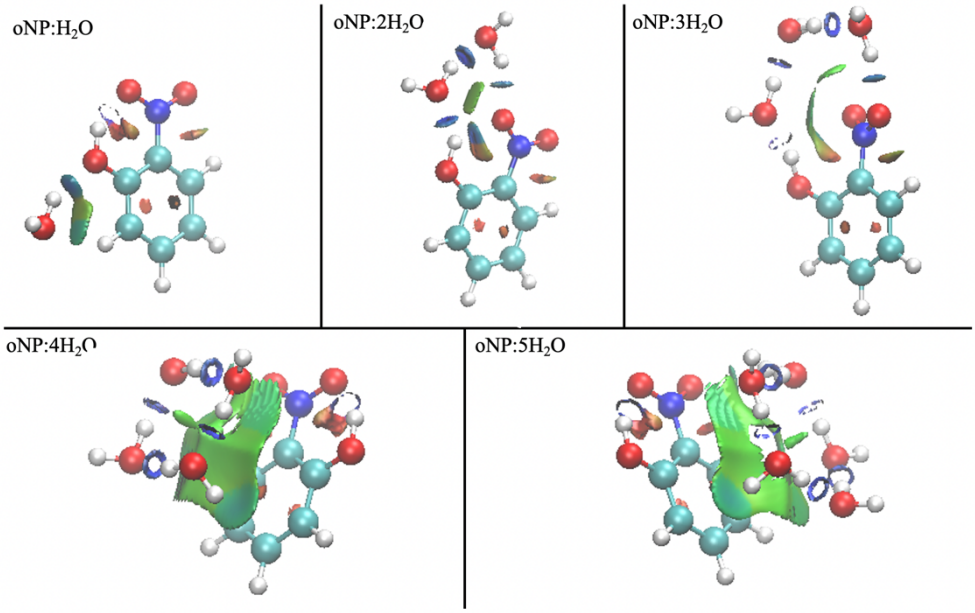

Figure 4*: NCIPlot renders showing noncovalent interactions in the lowest energy geometries of the oNP:nH_2O clusters.*

interaction between the functional groups becomes entirely repulsive in the 3H_2O complex. Additionally, oNP:3H_2O and oNP:4H_2O represent a turning point as water molecules are added around oNP where the hydrogen bonding network shifts away from heavily involving the chromophore. This is illustrated explicitly by the NCIPlot data. In the 3H_2O complex, the hydrogen bonding network observed qualitatively is clearly present, with the strong distortion of the chromophore geometry occurring to support the ideal geometry of the network of waters between the hydroxyl and nitro groups. Also contributing to the noncovalent network is a weak Van der Waals network between each water molecule in the network and the nitro group. The 4H_2O complex, on the other hand, shows strong hydrogen bonding between the water molecules in the cyclical network and a large Van der Waals surface between the water network and the aromatic π system of the chromophore. This confirms that the oNP molecule is not involved in the hydrogen bonding network in the higher-order clusters and explains the small geometrical distortion experienced by oNP relative to that it experiences with three waters present.

The theoretical geometries, vibrational spectra, and noncovalent interaction plots for the oNP:nH_2O clusters presented give a first approximation of the interfacial behavior of oNP and will provide deep insights when paired with the experimental VSFG data presented herein.

Infrared & Raman Results

To be active under VSFG spectroscopy, a vibrational mode must satisfy the selection rules for both infrared and Raman spectroscopy.[3] That is, the mode must cause a net change in both the dipole moment and molecular polarizability of the system. The IR selection rules much be satisfied so that the IR photon can be absorbed by the molecular vibration, and the Raman selection rules must be satisfied so that the visible photon is permitted to frequency mix with the IR photon

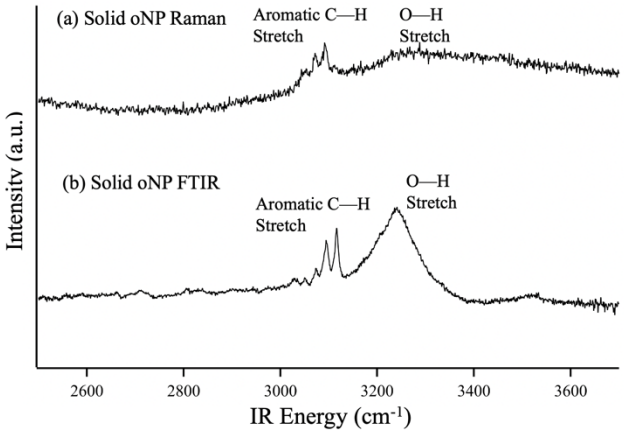

***Figure 5**: Raman (top) and FTIR (bottom) spectra of solid oNP verifying that the spectral features of interest are active under both techniques.*

to excite the molecule into the virtual excited state necessary to produce the sum-frequency photon.[8]

The vibrational modes of oNP that fall within the spectral region of interest in this study are the hydroxyl O—H stretch and the aromatic C—H stretches. To verify that these vibrational modes satisfy these criteria, both Raman and IR spectra were collected for solid oNP. The IR data was collected on an ATR-FTIR (attenuated total reflection-Fourier transform infrared) spectrometer and the Raman data on a Renishaw inVia Raman microscope and spectrometer. The spectra are presented in Figure 5. The two spectra both reveal the same modes: a broad O—H feature peaking at 3250cm^{-1} and four C—H features between 3000 and 3200cm^{-1}. This confirms that the target vibrational modes are both IR and Raman active and can therefore be expected to be detectable under VSFG spectroscopy.

Analysis of VSFG Spectra

Multiple VSFG spectra were collected in this study. Data was obtained for oNP in H_2O and D_2O using two different polarization combinations, yielding four spectra. An electromagnetic wave is polarized if it oscillates in a singular plane. In VSFG spectroscopy, manipulating the polarization of the two lasers determines the transition intensities for vibrational modes probed in the experiment. Beam polarizations are denoted as either S or P depending on the relationship between the plane in which they oscillate and the plane of incidence (depicted in Figure 6). An S polarized beam oscillates perpendicular to the plane of incidence, whereas a P polarized beam oscillates parallel to the plane of incidence.[3]

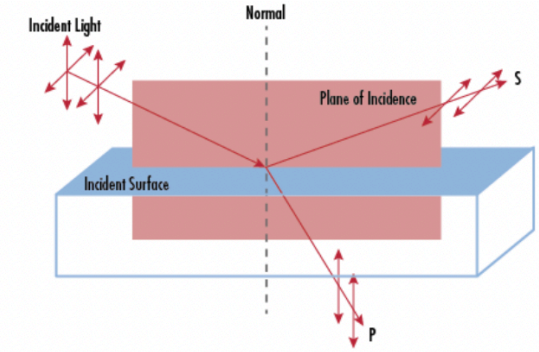

***Figure 6**: Illustration of the plane of incidence, interface, and S and P polarized light relative to them.*

The polarization combination defines the polarization of the input IR and visible photons as well as the output SFG photon and is reported in decreasing energy: sum-frequency, then visible, and finally infrared. There are four total polarization combinations available in VSFG spectroscopy: SSP, SPS, PSS, and PPP. SSP probes vibrational modes positioned perpendicular to the interface, SPS and PSS probe modes parallel to the interface, and PPP probes all mode of all orientations within the sample simultaneously. In this study, spectra were collected using SSP and PPP

polarizations and will thus be the focus of discussion.

Figure 7 shows the VSFG spectra collected for oNP in H_2O and D_2O, along with the assignments made for the important spectral features. The peaks represent the v=0 → v=1 transitions of oNP and interfacial solvent molecules when surrounded by either H_2O or D_2O, illuminating the behavior of this molecule at interfaces on the molecular level.

In both oNP/H_2O spectra, the highest frequency peak occurs at ~3680cm^{-1} and corresponds to the O—H vibrational mode on

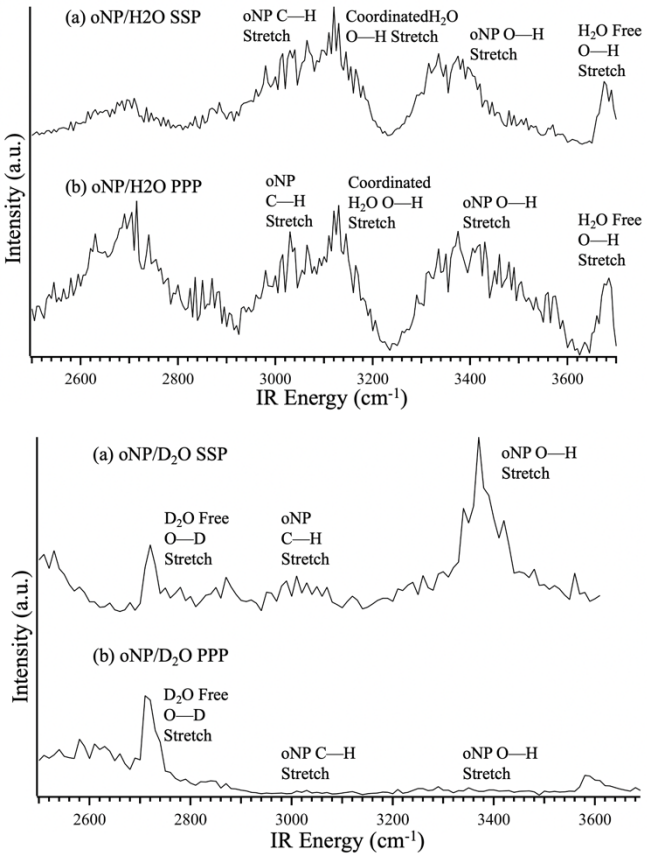

Figure 7*: SSP and PPP VSFG Spectra for oNP in H2O (top) and D2O (bottom). Spectral features corresponding to oNP and the interfacial solvent molecules have been labelled.*

H_2O molecules oscillating without the perturbation from a hydrogen bond (free O—H), a resonance that will be used as a reference point moving forward. The perturbation caused by hydrogen bonds has a stabilizing effect on vibrational modes, resulting in a redshift in vibrational frequencies. As such, the interfacial hydrogen bonded (coordinated) H_2O O—H mode is found at ~3120cm^{-1} in the spectra. The O—H vibrational mode of oNP is found between the two H_2O O—H modes at around 3400cm^{-1}, indicating that there is hydrogen bonding with surrounding H_2O molecules but to a lesser extent than the hydrogen bonding occurring between the interfacial H_2O molecules. Finally, the aryl C—H stretching modes of oNP are observed from 3000-3100cm^{-1}. The spectral features between the two polarization combinations are broadly the same, with the difference between the two being contained in linewidth and peak intensity. The PPP spectrum contains information about vibrational modes oscillating in all directions. Since the relative intensity are larger for the oNP O—H peak in the SSP spectrum than in the PPP spectrum, the comparison between the spectra confirms that the preferred orientation of oNP at the interface is with the functional groups perpendicular to the interface as shown in Figure 2. Thus, since it is more representative of the spatial orientation of oNP relative to the interface, the SSP spectrum will be used in further analysis due to its higher resolution and signal to noise.

The SSP oNP/D_2O spectrum contains the oNP O—H and aryl C—H spectral signatures in roughly the same frequency ranges as in the oNP/H_2O spectra. The free O—D stretching mode of D_2O appears at ~2720cm^{-1} appears in both spectra. The coordinated O—D stretch likely exists in interfacial D_2O, but it falls outside of the spectral window scanned in this experiment. Notably, the oNP vibrational frequencies do not appear with any significant intensity in the D_2O PPP spectrum, so it is not viable for use in analysis. The SSP D_2O spectrum, on the other hand, is highly useful since it strengthens the assignment of the oNP O—H stretch in the oNP/H_2O spectra by verifying that the feature at 3400cm^{-1} remains in the spectrum despite the lack of water molecules in the sample. Ultimately, the H_2O

spectra are of more importance to this study since they contain coordinated H_2O O—H features, which provide crucial information about interfacial hydrogen bonding networks and include more data about the interfacial vibrations of oNP.

Comparison to Theoretical Spectra

Theoretical vibrational spectra allow for highly precise spectral assignments since each vibrational frequency identified in the system can be visualized using the GaussView 6 software. The aim of this section is to identify the spectral region in which key spectral features (H_2O free O—H stretch, H_2O coordinated O—H stretch, oNP O—H stretch, and oNP C—H stretch) appear in the theoretical spectra for each oNP:nH_2O cluster and compare these locations to those of the same features in the experimental VSFG spectra. This will provide insight into the hydrogen bonding networks oNP is experiencing at interfaces, as well as its interfacial geometry.

The oNP/H_2O SSP VSFG spectrum is shown and the theoretical spectra for oNP:1-5H_2O with spectral assignments made using GaussView 6 underneath are shown in Figure 8. To allow the theoretical spectra to align with the experimental data, an empirical correction was applied to the calculated frequencies wherein the highest frequency belonging to the free OH stretch of water in each theoretical spectrum was forced to take on the same frequency as the free H_2O O—H stretch in the VSFG spectrum (3675cm^{-1}), shifting every other frequency into place. The oNP aromatic C—H stretches and the H_2O free O—H stretches appear in the same spectral region in each of the five theoretical spectra, shown with the colored rectangles in the figure. Of greater interest is the relative positions of the oNP O—H and the coordinated H_2O O—H frequencies.

In the VSFG spectrum, the assignments for the oNP O—H stretch is higher in energy than the hydrogen-bonded H_2O O—H stretch. However, for the oNP:nH_2O (n=1-3) theoretical spectra, the relationship is reversed. It is only in the n=4 and n=5 theoretical spectra that the two vibrational frequencies assume spectral positions that match their positions in

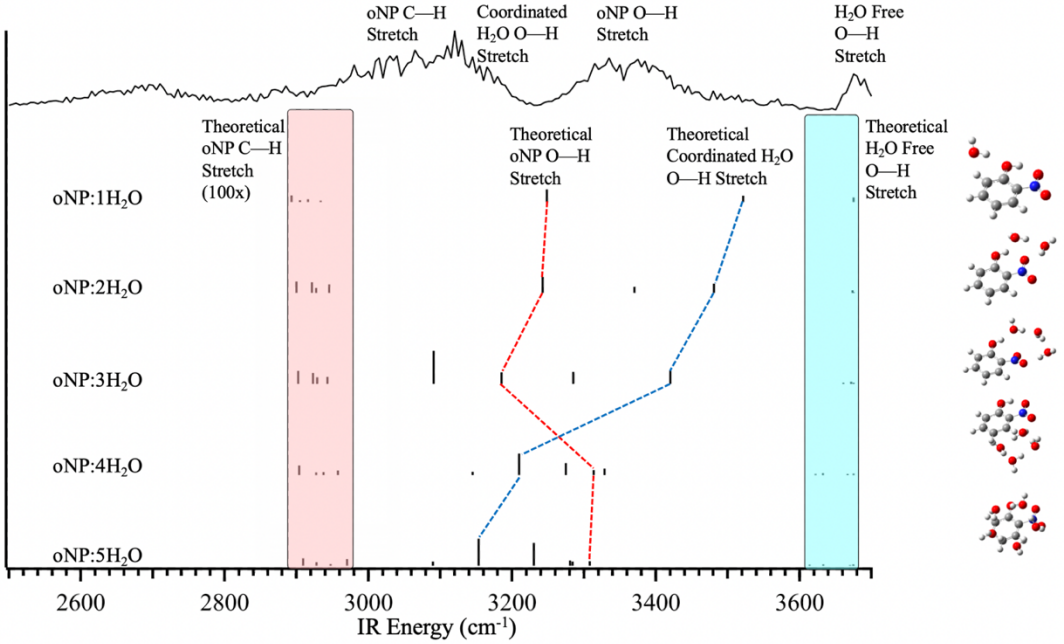

Figure 8*: Comparison between VSFG spectrum of oNP in H_2O (top) versus the vibrational spectra for the theoretical oNP:nH_2O geometries. Progression of the oNP O—H (red) and coordinated H_2O O—H (blue) vibrational modes as water molecules are added to the cluster is shown. The other black lines represent other, less significant coordinated H_2O O—H frequencies.*

the VSFG spectrum. The strong hydrogen bonding networks involving oNP that exist in the lower-order clusters redshift the oNP O—H stretching mode to such an extent that it does not align with the VSFG transition frequency observed in the experimental data. In the higher-order clusters, once the hydrogen bonding network involves the chromophore less heavily, the hydroxyl group oscillates relatively unperturbed at a frequency much closer to that observed at the oil-water interface. Furthermore, the coordinated water O—H stretch is higher in energy in the lower-order clusters since there is not particularly strong network of water molecules, and when the strong cyclical hydrogen bonding network between water molecules forms in the higher-order clusters, the mode becomes more redshifted and trades places with the oNP O—H frequency. Thus, the geometries found in the n=4 and n=5 water complexes are likely to be found at the interface. This was further confirmed by searching for alternate geometries for the higher order complexes, but no other structures with a significantly different geometry from the one indicated possessed an oNP O—H frequency matching any features in the VSFG spectrum.

Conclusion

The spectroscopic data presented, along with the theoretical calculations, provide evidence that *ortho*-nitrophenol is not heavily engaged in hydrogen bonding with its surrounding interfacial water molecules and is instead being supported by Van der Waals interactions between its aromatic π system and surrounding networks of hydrogen bonded solvent. This is indicated by the frequency of the oNP O—H stretch matching those of the theoretical structures possessing this type of noncovalent interaction. Furthermore, since oNP likely does not experience hydrogen bonding at the interface, its geometry remains in its unperturbed, planar form at the interface. This is further confirmed by the lack of experimental spectroscopic evidence of alternate geometries for the interfacial geometries identified.

The evidence presented here illuminates possible photochemical channels for nitroaromatic compounds. For instance, the photodissociation of oNP to produce nitric oxide requires planarity of the nitro group, something that would seem to be facilitated in the suggested interfacial geometry. This study has given a first approximation for the behavior of *ortho*-nitrophenol in particulate matter, and similar studies on the interfacial behavior of other nitroaromatic BrC molecules, such as para-nitrophenol, will be paramount in furthering the study of the solar absorption outcomes of BrC aerosol.

References

(1) Laskin, A.; Laskin, J.; Nizkorodov, S. A. Chemistry of Atmospheric Brown Carbon. *Chem. Rev.* **2015**, *115* (10), 4335–4382. https://doi.org/10.1021/cr5006167.

(2) Kusaka, R.; Nihonyanagi, S.; Tahara, T. The Photochemical Reaction of Phenol Becomes Ultrafast at the Air–Water Interface. *Nat. Chem.* **2021**, *13* (4), 306–311. https://doi.org/10.1038/s41557-020-00619-5.

(3) Carpenter, A. P. Molecular Structure and Bonding at Nanoemulsion Surfaces. Ph.D, University of Oregon, Eugene, OR, 2020.

(4) Frisch, M. J et al. Gaussian 16, Revision C.01, 2016.

(5) Zhang, J.; Dolg, M. ABCluster: The Artificial Bee Colony Algorithm for Cluster Global Optimization. *Phys. Chem. Chem. Phys.* **2015**, *17* (37), 24173–24181. https://doi.org/10.1039/C5CP04060D.

(6) Kidwell, N. M et al. Nonstatistical Dissociation Dynamics of Nitroaromatic Chromophores. *J. Phys. Chem. A* **2019**, *123* (19), 4262–4273. https://doi.org/10.1021/acs.jpca.9b02312.

(7) Yang, W et al. NCIPLOT: A Program for Plotting Non-Covalent Interaction Regions. *J Chem Theory Comput* **2011**, *7* (3), 625–632. https://doi.org/10.1021/ct100641a.

(8) *Tutorials in vibrational sum frequency generation spectroscopy. I. The foundations | Biointerphases | AIP Publishing*. https://pubs.aip.org/avs/bip/article/17/1/011201/2835334/Tutorials-in-vibrational-sum-frequency-generation (accessed 2024-04-01).